



## Glycine-Induced Hydrothermal Synthesis of Carbonated Hydroxyapatite Nanorods with Luminescence Property†

JINSONG XIE<sup>1,2,\*</sup>, CHANGAN TIAN<sup>1,2</sup>, HONGDIAN LU<sup>1,2</sup>, DIFANG ZHAO<sup>1,2</sup> and MING DING<sup>1,2</sup>

<sup>1</sup>Department of Chemistry and Materials Engineering, Hefei University, Hefei 230022, P.R. China

<sup>2</sup>Key Lab of Powder and Energy Sources Materials, Hefei University, Hefei 230022, P.R. China

\*Corresponding author: E-mail: xjs153@hfu.edu.cn

AJC-11320

In the article, carbonated hydroxyapatite nanorods with a length around 500 nm and a diameter about 100 nm were synthesized, utilizing an easy glycine-assisted hydrothermal technique. The structures and morphologies of the as-obtained products were characterized by powder X-ray diffraction, field emission scanning electron microscopy and Fourier transform infrared spectroscopy (FTIR). Additionally, the optical properties of the products, such as UV-visible absorption and photoluminescence properties were preliminarily studied.

**Key Words:** Glycine-induced hydrothermal synthesis, Carbonated hydroxyapatite, Nanorod, Optical properties.

### INTRODUCTION

Recently, as a kind of biomedical material, hydroxyapatite (HA) with the components of  $\text{Ca}_5(\text{PO}_4)_3\text{OH}$  or  $\text{Ca}_{10}(\text{PO}_4)_6(\text{OH})_2$  has drawn much attention because of its wide application in drug delivery<sup>1</sup>, protein chromatography<sup>2</sup>, catalysis<sup>3</sup> and so on. As the same time, owing to the properties of hydroxyapatite depending on its morphologies and components, there are increasing studies on the synthesis of hydroxyapatite with morphologies by different mild techniques, such as biomimetic process<sup>4</sup>, hydrothermal method<sup>5</sup>, microemulsions<sup>6</sup>, flux strategy<sup>7</sup>. However, there are few reports on carbonated hydroxyapatite,  $\text{Ca}_{10}(\text{PO}_4)_6(\text{CO}_3)_2(\text{OH})_2$ , which is usually classified as A type (substitution of  $\text{CO}_3^{2-}$  for  $\text{OH}^-$ ) and B type (substitution of  $\text{CO}_3^{2-}$  for  $\text{PO}_4^{3-}$ )<sup>4</sup>. For instance, Xiao *et al.*<sup>8</sup> constructed a family of orderly arranged textures composed of two-dimensional nanoscale carbonated hydroxyapatite in presence of succinylated gelatin and cetyltrimethyl ammonium bromide. Zhang *et al.*<sup>5</sup> fabricated carbonated hydroxyapatite nano and microcrystals with multiform morphologies, which have strong self-activated luminescence properties.

Herein, we demonstrated a simple glycine-assisted hydrothermal technique to prepare carbonated hydroxyapatite nanorods with uniform morphology. The precursor of glycine plays a double-role in the reaction procedure, not only acting as template to induce the formation of the one-dimensional nanorods, but also supplying the  $\text{OH}^-$  and  $\text{CO}_3^{2-}$  resources.

Furthermore, the as-obtained products showed excellent optical absorbance and photoluminescence properties, which may be potentially applied in optical devices.

### EXPERIMENTAL

All the chemicals were of analytical grade reagents and used without further purification. In a typical preparation carbonated hydroxyapatite nanorods procedure, 2 mmol of  $\text{Ca}(\text{NO}_3)_2 \cdot 4\text{H}_2\text{O}$ , 20 mmol of glycine, 1.2 mmol of  $\text{Na}_2\text{HPO}_4 \cdot 12\text{H}_2\text{O}$  and 15 mL deionized water were transferred into a Teflon-lined stainless steel autoclave with a capacity of 25 mL. The autoclave was maintained in a digital-type temperature-controlled oven at 180 °C for 18 h. As the autoclave cooled to room temperature naturally and then, the as-obtained products were centrifuged, washed, respectively with absolute ethanol and deionized water three times and finally dried at 60 °C for 5 h.

XRD pattern of sample was measured on a Bruker D8-advance X-ray diffractometer with  $\text{CuK}\alpha$  radiation ( $\lambda = 0.154056$  nm). FE-SEM images and EDS spectrum were measured on a Hitachi S-4800 field emission scanning electron microanalyser employing an operating voltage of 10 kV.

The FTIR spectrum was recorded on a Bruker Vector-22 FT-IR spectrometer from 4000-400  $\text{cm}^{-1}$ . UV-Visible absorption spectrum and room temperature photoluminescence spectrum were characterized on an Agilent 8453 UV-visible spectro-

†Presented to The 5th Korea-China International Conference on Multi-Functional Materials and Application.

photometer and a Perkin-Elmer LS55 fluorescence spectrophotometer.

## RESULTS AND DISCUSSION

The typical XRD pattern of the obtained product is shown in Fig. 1a. All the diffraction peaks can be easily indexed as a pure hexagonal carbonated hydroxyapatite phase with space group P63/m (176) and refined lattice constants  $a = 9.418$  and  $c = 6.883$  Å, which matches well with the standard data in JCPDS card No. 21-0145. The EDS spectrum as shown in Fig. 1b confirms the presence of Ca, P, O and C from the sample. Additionally, the observed Au peaks in the above EDS spectrum attributed to the coating for SEM analysis. The FTIR of the sample is shown in Fig. 1c, the peaks at 564, 603  $\text{cm}^{-1}$  are assigned to the bending vibrations of  $\text{PO}_4^{3-}$  groups; the peaks at 1100, 1030  $\text{cm}^{-1}$  are due to the asymmetric stretching vibrations of  $\text{PO}_4^{3-}$  groups<sup>9</sup>. The peaks at 3570, 633  $\text{cm}^{-1}$  are attributed to  $\text{OH}^-$  ion. The broad peak at 3420 belonged to the O-H vibration of  $\text{H}_2\text{O}$  in the sample. In addition, the peaks at 1460 and 1380  $\text{cm}^{-1}$  are from  $\text{CO}_3^{2-}$ , indicating the sample is mainly B type substitution<sup>8</sup>. Furthermore, the peak at 1640  $\text{cm}^{-1}$  is due to the bond formation between  $\text{CO}_3^{2-}$  groups and  $\text{Ca}^{2+}$  ion<sup>10</sup>. The above experimental results indicate that the as-obtained product is B-type carbonated hydroxyapatite.

Fig. 2a shows the FESEM image with a low magnification. It can be seen that the product is composed of large-scale regular

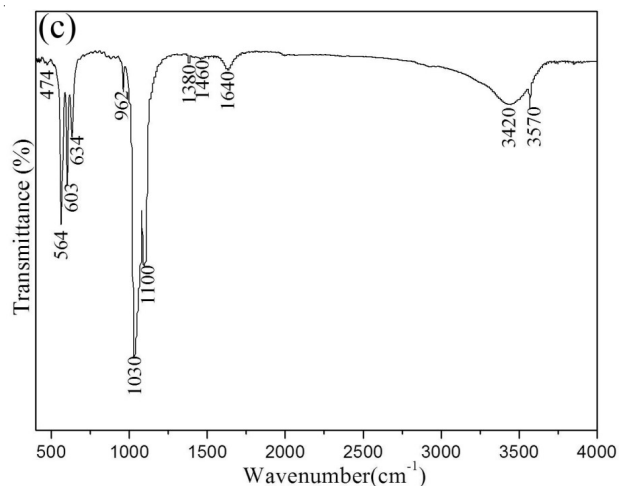
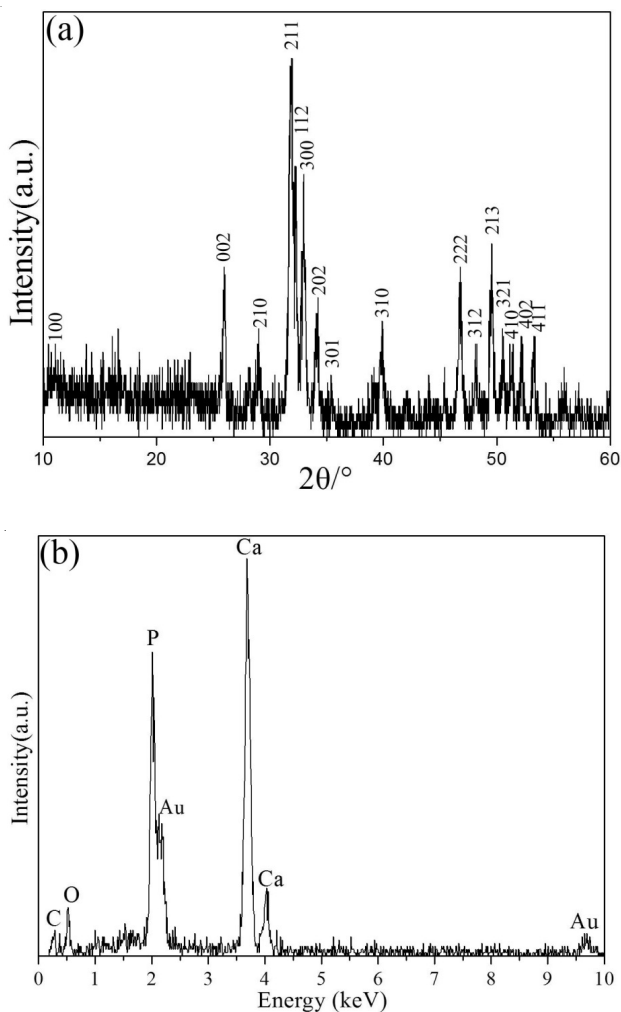


Fig. 1. (a) XRD pattern, (b) EDS spectrum and (c) FTIR spectrum of the as-obtained product

leaf-like particles. The further magnified FESEM image shows that the product indeed displays a rod-like with a length around 500 nm and a diameter about 100 nm. The UV-visible spectrum of the product is shown in Fig. 3a, the obtained product has a wide and intense absorbance peak in the region of 300-550 nm, which may be ascribed to the reduced size of materials. Fig. 3b illustrates the photoluminescence spectrum of the as-prepared product at room temperature. The emission spectrum consists of three main emission bands, one is strong and broad green band at 576 nm, other weak bands are around 536 and 720 nm, respectively, which may be associated with the  $\text{CO}_2^{\cdot-}$  radical impurities in the crystal lattice of the carbonated hydroxyapatite<sup>5</sup>. However, the accurate photoluminescence mechanism is still further investigated.

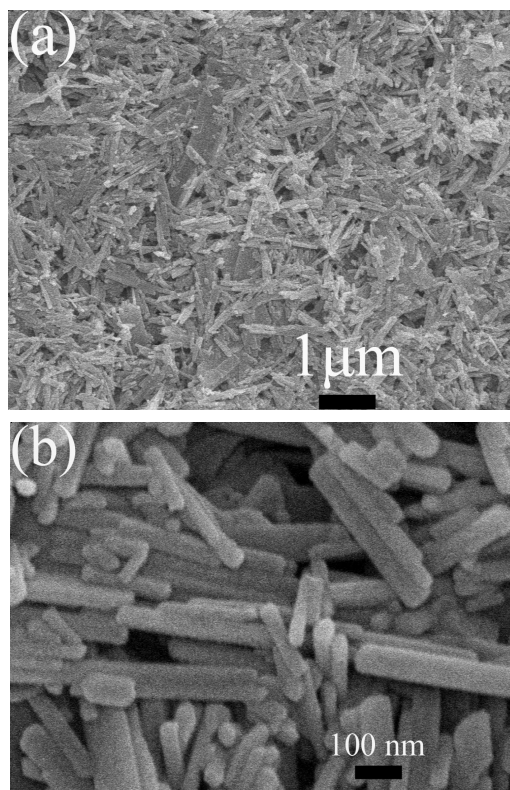


Fig. 2. (a) low magnification and (b) high magnification FESEM images of as-obtained product

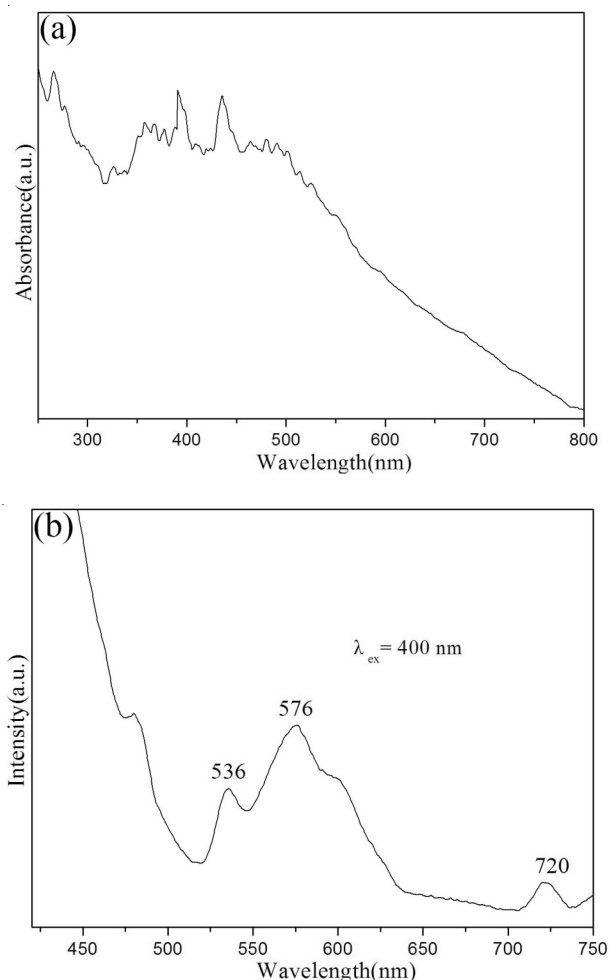


Fig. 3. (a) UV-Visible spectrum and (b) photoluminescence spectrum of as-obtained product

### Conclusion

In summary, we successfully fabricate carbonated hydroxyapatite nanorods through glycine-induced hydrothermal

method. The component and morphology were determined by a series of analytic methods. The experimental results indicate the rod-like B-type carbonated hydroxyapatite has good UV-visible absorbance ability and intense green emission luminescence properties, which may be applicable in optical devices.

### ACKNOWLEDGEMENTS

This work was supported by the Natural Science Foundation of Education Department of Anhui Province (KJ2012B154), the Natural Science Foundation of Hefei University (12RC02) and the National Natural Science Foundation of China (51102073), the Natural Science Foundation of Anhui Province (10040606Q53, 11040606M100).

### REFERENCES

1. M.P. Ginebra, T. Traykova and J.A. Planell, *J. Control. Rel.*, **113**, 102 (2006).
2. M. Wakamura, K. Hashimoto and T. Watanabe, *Langmuir*, **19**, 3428 (2003).
3. J. Xu, T. White, P. Li, C.H. He and Y.F. Han, *J. Am. Chem. Soc.*, **132**, 3172 (2010).
4. L.C. Palmer, C.J. Newcomb, S.R. Kaltz, E.D. Spoerke and S.I. Stupp, *Chem. Rev.*, **108**, 4754 (2008).
5. C.M. Zhang, J. Yang, Z.W. Quan, P.P. Yang, C.X. Li, Z.Y. Hou and J. Lin, *Crys. Growth Des.*, **9**, 2725 (2009).
6. K. Wei, Y.J. Wang, C. Lai, C.Y. Ning, D.X. Wu, G. Wu, N.R. Zhao, X.F. Chen and J.D. Ye, *Mater. Lett.*, **59**, 220 (2005).
7. K. Teshima, S.H. Lee, M. Sakurai, Y. Kamenoi, K. Yubuta, T. Suzuki, T. Shishido, M. Endo and S. Oishi, *Crys. Growth Des.*, **9**, 2937 (2009).
8. J.W. Xiao, Y.C. Zhu, Q.C. Ruan, Y.Y. Liu, Yi Zeng, F.F. Xu and L.L. Zhang, *Crys. Growth Des.*, **10**, 1492 (2010).
9. A. Doat, M. Fanjul, F. Pelle, E. Hollande and A. Lebuglem, *Biomaterials*, **24**, 3365 (2003).
10. M.F. Chen, J.J. Tan, Y.Y. Lian and D.B. Liu, *Appl. Surf. Sci.*, **254**, 2730 (2008).